

Preparation of fibrous sodium titanate and its adsorption property toward neutral red, methylene blue, malachite green and crystal violet

JI-GUO HUANG^a, MEI-XIA ZHAO^a, HAI-TAO CHEN^a, LI-LI DONG^{b,c,*}, XUE-TING GUO^a, XING-JUAN LIU^a

^aKey Laboratory of Groundwater Resources and Environment, Ministry of Education, Jilin University, Changchun 130026, PR China

^bKey Laboratory of Songliao Aquatic Environment, Ministry of Education, Jilin Jianzhu University, Changchun 130118, PR China

^cSchool of Environment, Northeast Normal University, Changchun 130117, PR China

Fibrous sodium titanate was prepared with the reaction of Ti plates, NaOH and H₂O₂ at 80°C for 24h. Sodium titanate was characterized by XRD, FT-IR, SEM. Sodium titanate prepared exhibited excellent adsorption capability for neutral red (NR), methylene blue (MB), malachite green (MG) and crystal violet (CV), and the saturated adsorption capacities were 323.42, 235.18, 261.38 and 206.92 mg/g at 25°C, respectively. The pseudo-second-order kinetic model and Langmuir model could well describe the adsorption of NR, MB, MG and CV. This work is of great significance for applications of sodium titanate as a promising adsorbent material for dyeing water purification.

(Received October 1, 2014; accepted March 19, 2015)

Keywords: Na₂Ti₃O₇, Cationic dyes, Adsorption

1. Introduction

Cationic dyes are extensively used in industry, leading to the increase of the discharge of dye to the water [1]. The dyeing wastewater reduces the solar light penetration and retards the photosynthetic activity of aquatic plant [2]. In addition, the colored effluence also triggers an increasing toxicity and carcinogenic, which threatens the water security for human and animals [3]. This resulted in a demand to remove the dyes from effluents. Therefore the treatment of cationic dyes raised much attention. To date, a number of chemical, physical, and biological methods have been developed for removing dyes from waste water. Among them, adsorption technique is believed to be one of the most effective and simplest processes, and various adsorbents have been tested to remove dyes from water [2, 4, 5]. For example, activated carbon has been regarded as an excellent adsorbent and used widely. However, it was sometimes treated as one-off adsorbent due to the high regeneration cost [6, 7]. This has led to the search for more efficient and cheaper alternate adsorbents. In recent year, there has been an increasing interest in the utilization of titanate in environmental studies [8-11]. It had been found that titanate play the roles of adsorbent and photocatalyst simultaneously in the removal of dyes [12, 13]. Consequently, they are considered as promising

adsorbents for dye removal. Moreover, procedures of different ways to prepare titanate are relatively complex or need a relatively high temperature [12-15] which increase the cost, so an easy way to prepare the titanate is necessary.

In this work, we successfully prepared fibrous sodium titanate through a simple hydrothermal reaction between Ti plate and the mixed solution of NaOH and H₂O₂ at just 80°C for 24h. The adsorption capabilities for cationic dyes of sodium titanate were studied. The adsorption kinetic and isotherm was studied. It has been known that sodium titanate with low crystallinity was a promising adsorbent material for dyeing water treatment. So this work is of great significance.

2. Experimental

2.1. Materials

Cold-rolled titanium plate, 99.5% in purity, was purchased from Baoji Fuxin Nonferrous Metal Products Co., Ltd, China. Hydrochloric acid (37%), sodium hydroxide (NaOH) and nitric acid (67%) were purchased from Beijing Chemical Works. Hydrofluoric acid (40%) was purchased from Tianjin Chemical Reagent Research Institute. Hydrogen peroxide (30%) was obtained from

Xilong Chemical Co., LTD (China). Methylene blue (MB), neutral red (NR), crystal violet (CV), basic red 2 (BR2), rhodamine B (RhB) and methyl orange (MO) were obtained from Tianjin Guangfu Fine Chemical Research Institute (China). Malachite green (MG) was obtained from Tianjin Bodi Chemical Co., Ltd. All reagents were of analytical grade. The water used was distilled.

2.2. Preparation

The sodium titanate was prepared according to the procedures described in literature [16]. After picking and ultrasonically cleaning in distilled water, each two pieces of cleaned Ti plates (5cm×5cm×0.2mm) were soaked in a Teflon-lined stainless steel autoclave with a mixed solution (volume ratio of NaOH solution (10mol/L) and hydrogen peroxide (30%) was 1:1). The autoclave was kept at 80°C with 24h and cooled to room temperature. The remaining titanium plates were took out for reuse. 1mol/L hydrochloric acid was added gradually to adjust the pH to 7 of the solution. Precipitates were washed for several times and then dried by water bath at 40°C.

2.3. Characterization

XRD patterns were acquired on an X-ray diffraction spectrometer (BRUKER axs D8 ADVANCE, Cu K α , $\lambda=1.54056$ Å). FT-IR curves were recorded on SHIMADZU 8400s Fourier transform infrared spectrometer. The SEM images were recorded with a scanning electron microscopy (SEM, HITACHI-SU8000) at room temperature. The specific surface area was calculated from the N₂ adsorption isotherm using the Brunauer–Emmett–Teller (BET) method, and the pore size distribution was determined using the Barrett–Joyner–Halenda (BJH) mathematical model. The sample was degassed at 50°C for 12 h before test.

2.4 Adsorption test

All the adsorption experiments were conducted under stirring at room temperature (25°C) in the dark. The general experimental process is described as follows: 0.2g of the sample was added to 200ml of dye solution with certain initial concentration without pH adjustment. At appropriate time intervals, the aliquots were withdrawn from the suspension and the adsorbents were separated from the suspension via centrifugation. SDPTOP UV 2600PC spectrophotometer was adopted to measure the concentration of residual dyes at the corresponding maximum absorption (Table 1). The concentration of phenol was measured by 4-aminoantipyrine spectrophotometric method at 510nm wavelength [17].

Table 1. Maximum absorption wavelengths of different substance.

Category	Name	Maximum absorption wavelength/nm
Cationic dyes	Neutral red (NR)	523
	Malachite green (MG)	621
	Methylene blue (MB)	664
	Crystal violet (CV)	590
	Basic red 2 (BR2)	530
	Rhodamine B (RhB)	554
Anionic dyes	Methyl orange (MO)	464
Organic	Phenol	510

3. Results and discussion

3.1 Characterization results of sodium titanate

The sample prepared in aqueous solution containing NaOH (10M) and H₂O₂ (30%), at just 80°C for 24h. As shown in Fig. 1, It can be seen that the typical morphology of the sample was consisted of a large number of nanowires with a diameter of 40-50nm and a length of several hundred nanometers.

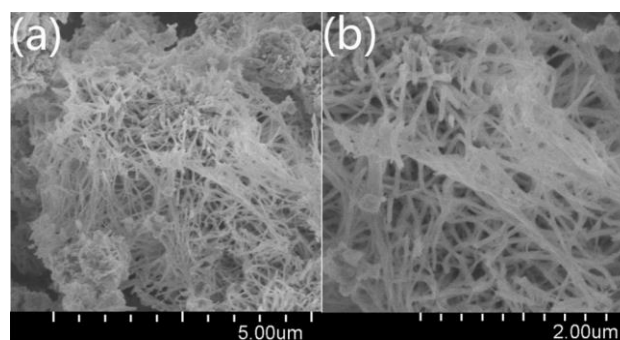


Fig. 1. SEM images of the sample.

XRD patterns of the sample and the Ti plate after pretreatment are shown in Fig. 2. The absence of any Ti peaks in the sample pattern indicated a high degree of conversion during the hydrothermal process. The XRD pattern of sample exhibited a strong peak around 10° and the other three weak broad peaks around 24.5°, 28.34° and 48.3°, which are characteristic of Na₂Ti₃O₇ (JCPDS no. 72-0148) with low crystallinity [14, 18].

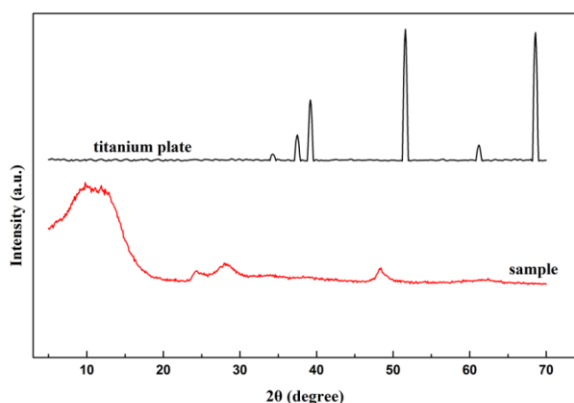


Fig. 2. XRD patterns of metal Ti plate and the sample.

As shown in Fig. 3, the presence of Ti-OH and hydroxyl groups adsorbed on the surface of samples were confirmed by the appearance of broad intense bands at 3404 cm^{-1} and 3242 cm^{-1} [13, 19], respectively. The characteristic bands around 1630 cm^{-1} and 1385 cm^{-1} could be assigned to H-O-H binding vibration mode and the Ti-O vibrations [13]. The peak at 900 cm^{-1} was resulted in the peroxy groups provided by O_2^{2-} adsorbed on the surface of the sample [20, 21]. The wide band at 460 cm^{-1} in the sample spectra can be assigned to the crystal lattice vibration of TiO_6 octahedra which is the topic structure of the crystalline $\text{Na}_2\text{Ti}_3\text{O}_7$ [19, 22]. Combined with the result of XRD, it confirmed that the sample was $\text{Na}_2\text{Ti}_3\text{O}_7$ (sodium titanate) with low crystallinity and the surface of it was dominated by negative hydroxyl groups.

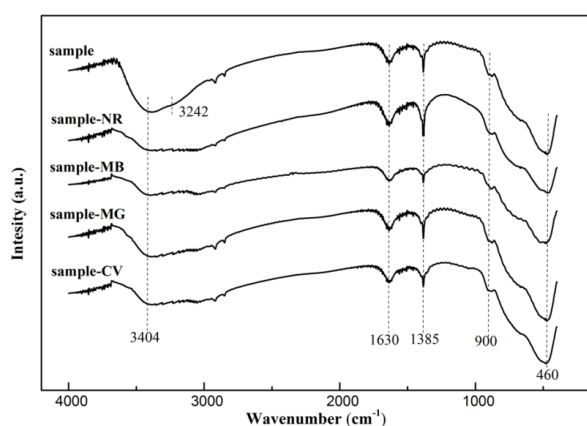


Fig. 3. FT-IR spectra of the sample and dyes adsorbed on sample.

The N_2 adsorption-desorption isotherm of sodium titanate indicated a specific surface area of $31.93\text{ m}^2/\text{g}$ by BET analysis. The corresponding BJH analysis (curve inserted) suggested a predominant pore diameter

distribution of 14.2 nm and a total pore volume of $0.210\text{ cm}^3/\text{g}$. The BJH result indicated that the sample belonged to mesoporous material. Pores presumably arise from the space between the stacked filaments of $\text{Na}_2\text{Ti}_3\text{O}_7$, and this is likely to benefit the adsorption performance [23].

3.2. Adsorption experiment

Eight different substrates including MB, MG, CV, NR, BR2, RhB, MO and phenol were used to study the adsorption property of sodium titanate. As can be seen from Fig. 4, sodium titanate showed great adsorption effect on four cationic dyes including NR, MG, MB and CV, but had no effect on BR2, RhB, MO and phenol. Therefore, the sample may have selective adsorption property on some cationic dyes (NR, MG, MB and CV). Combined with the FT-IR characterization results, as the surface was dominated by negative hydroxyl groups [24, 25], sodium titanate presented good selective adsorption property toward some cationic dyes but not all.

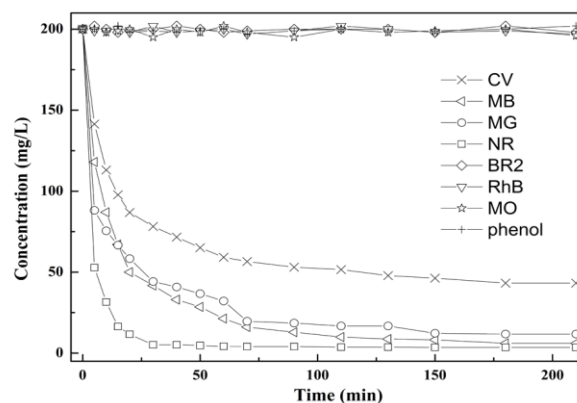


Fig. 4. Concentration of different substances solutions with the sample (initial concentration 200 mg/L , sodium titanate dosage 1.0 g/L).

It can be seen from Fig. 5, molecular structures of NR, MG, MB and CV have the same characteristics: (1) The positive charge of the dye is localized and isolated from the main part of the dye; (2) Two methyls or hydrogens hold small space bind to positive charge of the dye. Two ethyls bound to positive charge of RhB occupied a larger space than that of two methyls, hindering the electrostatic attraction between RhB and the sodium titanate. As the positive charge of BR2 was surrounded by the entire molecule, it was impossible for BR2 to be absorbed by sodium titanate through electrostatic attraction. Sodium titanate presented good selective adsorption property toward these cationic dyes whose positive charger was relatively bare. In addition, the adsorption rates on NR, MG, MB and CV were

different (NR>MB>MG>CV). Seen by Fig. 5, as the charge was same to each other, the smaller the size of the molecular is, the easier the adsorption is.

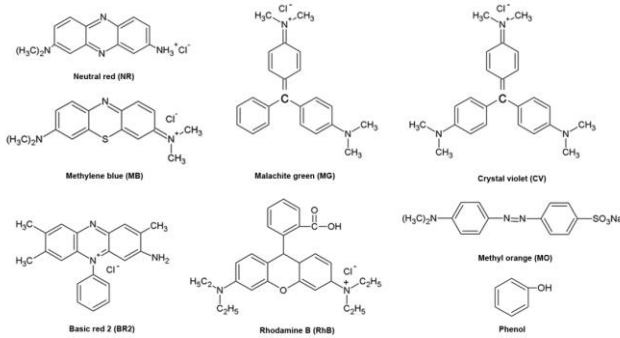


Fig. 5. Formulae of NR, MB, MG, CV, BR2, RhB, MO and phenol.

As seen from Fig. 6, the concentration of NR (the same to MB, MG and CV) decreased dramatically in the first 5min. This was due to the strong electrostatic interaction between positively charged NR (the same to MB, MG and CV) and negatively charged sodium titanate [26-29]. Subsequently, the concentration of NR (the same to MB, MG and CV) slowed down with the extension of the adsorptive time. The adsorption rate was slower than that at the beginning stage. It could be explained that the decreasing adsorption points and vacant surface became more difficult to be occupied with reaction advanced, due to the repulsion between adsorbed NR (the same to MB, MG and CV) molecules [13]. The result also showed that the experimental saturated adsorption capacities for NR, MG, MB and CV were 323.42, 235.18, 261.38 and 206.92 mg/g at 25°C, respectively.

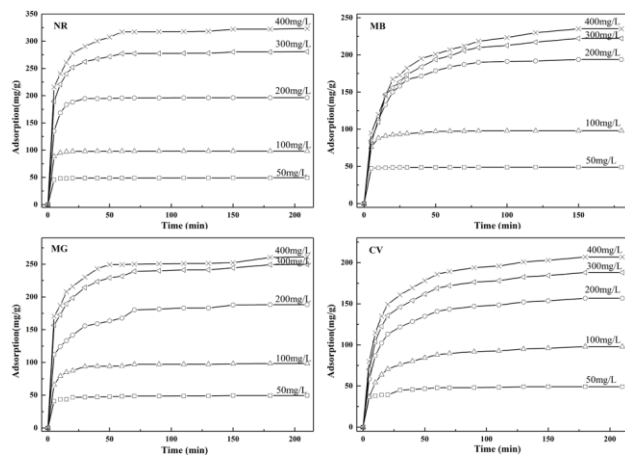


Fig. 6. The adsorption curves of NR, MB, MG and CV at different initial concentration (sodium titanate dosage 1.0g/L).

In order to investigate the mechanism and

characteristics of sodium titanate adsorption in the dyes' removal, the linear plots of pseudo-first-order and pseudo-second-order kinetic models [30] are showed in Fig. 7 and Fig. 8 respectively, and the adsorption kinetic parameters related to models are figured out in Table 2. It can be seen that the trend line of the pseudo-first-order model deviated obviously from the experimental data, but the trend line of the pseudo-second-order model passed through the whole experimental data. Correspondingly, the correlation coefficient values of pseudo-first-order model were lower than that of pseudo-second-order model which were higher than 0.9993. The values of $q_{e,cal}$ estimated from pseudo-second-order model were comparable with the experimentally determined values of $q_{e,exp}$, which indicated a better applicability of pseudo-second-order model to the adsorption of NR (the same to MB, MG and CV) in this study. It also suggested that the rate of the adsorption process was controlled by the chemical adsorption, which involved valence forces through sharing or exchange of electrons between adsorbent and adsorbate [23, 31].

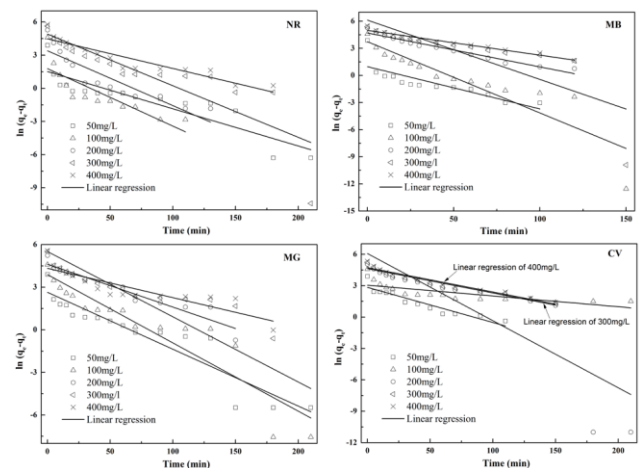


Fig. 7. Pseudo-first-order kinetic plots for NR, MB, MG and CV.

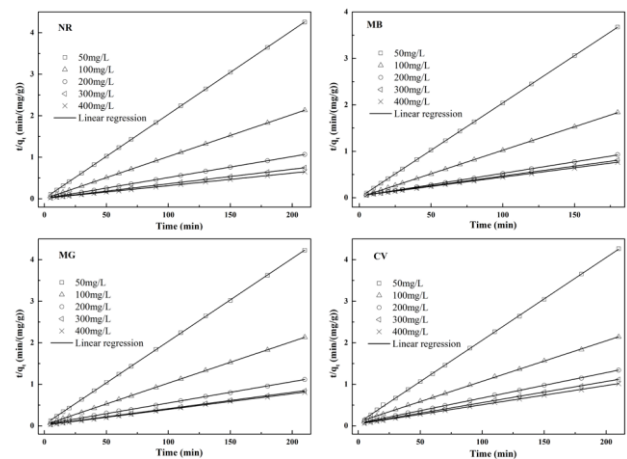


Fig. 8. Pseudo-second-order kinetic plots for NR, MB, MG and CV.

Table 2. Equations and parameters of kinetic models and kinetic parameters of dyes onto sodium titanate.

Kinetic model		Pseudo-first-order kinetic model				Pseudo-second-order kinetic model		
Equation		$\ln(q_e - q_t) = \ln q_e - k_1 t$				$t/q_t = (1/q_e) t + 1/(q_e^2 k_2)$		
Capacity term		q_t, q_e : the amounts of dyes adsorbed (mg/g) at time t and at equilibrium, respectively; k_1 : the first-order equilibrium rate constant (min^{-1}); k_2 : the second-order equilibrium rate constant ($\text{g}/(\text{mg}\cdot\text{min})$).						
Parameters	$q_{e,\text{exp}}$ (mg/g)	$q_{e,\text{cal}}$ (mg/g)	k_1 (min^{-1})	R_1^2	$q_{e,\text{cal}}$ (mg/g)	k_2 ($\text{g}/(\text{mg}\cdot\text{min})$)	R_2^2	
Concentration of NR (mg/L)	50	49.36	4.54	0.0337	0.78629	49.43	0.000270	0.99999
	100	98.40	5.92	0.0520	0.68576	98.52	0.000058	1.00000
	200	196.46	29.84	0.0496	0.80449	198.02	0.000008	0.99994
	300	281.02	135.22	0.0467	0.70762	284.09	0.000003	0.99996
	400	323.42	87.91	0.0268	0.85990	328.95	0.000002	0.99991
Concentration of MB (mg/L)	50	49.01	2.63	0.0468	0.65786	49.07	0.000429	1.00000
	100	97.98	41.84	0.0718	0.79887	98.72	0.000027	0.99997
	200	193.93	109.00	0.0375	0.95780	202.84	0.000005	0.99975
	300	222.26	452.51	0.0655	0.62166	235.85	0.000003	0.99974
	400	235.18	145.73	0.0274	0.96353	249.38	0.000003	0.99949
Concentration of MG (mg/L)	50	49.65	14.03	0.0401	0.86848	50.05	0.000151	0.99995
	100	98.39	48.70	0.0481	0.84329	99.60	0.000026	0.99996
	200	188.22	101.18	0.0302	0.91430	194.55	0.000006	0.99933
	300	249.78	246.87	0.0459	0.63684	254.45	0.000003	0.99973
	400	261.38	75.89	0.0207	0.76942	263.85	0.000003	0.99950
Concentration of CV (mg/L)	50	49.22	17.01	0.0335	0.86471	50.18	0.000140	0.99980
	100	97.97	20.89	0.0103	0.56623	102.46	0.000031	0.99979
	200	156.76	431.49	0.0641	0.70554	163.93	0.000006	0.99979
	300	188.11	101.94	0.0233	0.94854	196.85	0.000006	0.99979
	400	206.92	111.75	0.0232	0.94903	215.98	0.000005	0.99978

Table 3. Isotherms coefficients according to Freundlich and Langmuir.

Elements	$q_{\text{max,exp}}$ (mg/g)	Freundlich			Langmuir		
		$q_e = k_f C_e^{1/n}$			$q_e = q_{\text{max}} C_e / (A + C_e)$		
		k_f (mg/g)	n	R^2	q_{max} (mg/g)	A mg/L	R^2
NR	323.42	0.4415	6.17×10^{-5}	0.80721	337.84	3.5000	0.99960
MB	235.18	0.3469	7.53×10^{-6}	0.66665	238.10	3.1548	0.99931
MG	261.38	0.2977	4.94×10^{-7}	0.92990	266.67	3.0880	0.99942
CV	206.92	0.2504	7.45×10^{-8}	0.89134	208.77	6.6263	0.99259

The adsorption process was further studied by two classical isotherm models, Langmuir and Freundlich [32], as shown in Fig. 9. Their corresponding equations and parameters for adsorption of dyes onto the sample are listed in Table 3. It can be seen that the Langmuir model is quite suitable to the adsorption, and the correlation coefficients are higher than 0.99. In addition, the q_{max} of NR, MB, MG and CV calculated through the Langmuir model were 337.84, 238.10, 266.67 and 208.77, this in accord with the q_{max} come from the experiment. Combined with the FT-IR characterization results, after the absorption of NR, MB, MG and CV, the band at

3242cm^{-1} of the sample almost disappeared, which means that the amount of hydroxyl groups decreased and even disappeared. This further confirmed that the sodium titanate prepared presented good selective adsorption property toward NR, MB, MG and CV through the strong electrostatic interaction, and the adsorption was single layer adsorption according to the Langmuir model.

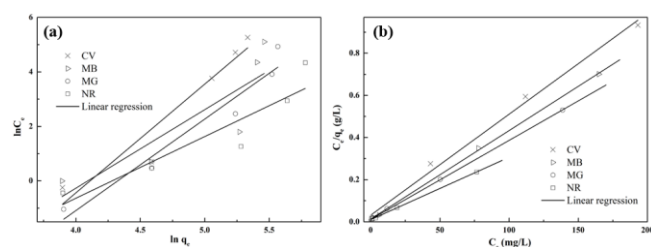
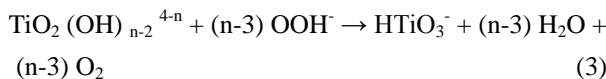
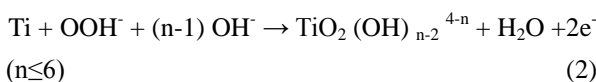


Fig. 9. Langmuir and Freundlich sorption isotherms of NR, MB, MG and CV on sodium titanate.

3.3 Reaction and absorption mechanism

The generation and absorption mechanism of sodium titanate was proposed. In alkaline solution, dissociation of H_2O_2 formed the OOH^- ion in Equation (1). It reacted with Ti to form a metastable and highly soluble peroxide complex $(\text{TiO}_2(\text{OH})_{n-2}^{4-n})$ [20]. Then reaction (3) took place immediately to generate HTiO_3^- in the case of excess OOH^- ions. The $\text{Na}_2\text{Ti}_3\text{O}_7$ generated [16] at last with hydroxyl groups on the surface of it. Thus the $\text{Na}_2\text{Ti}_3\text{O}_7$ was negative, so it could absorb the cationic dyes such as NR^+ , MB^+ , MG^+ and CV^+ .



C^+ represents cationic dyes such as NR^+ , MB^+ , MG^+ and CV^+ .

4. Conclusion

Fibrous sodium titanate with low crystallinity was prepared with the reaction of Ti plates, NaOH and H_2O_2 at 80°C with 24h. As the surface was dominated by hydroxyl groups, it exhibited excellent adsorption capability for some cationic dyes whose positive charge is relatively bare such as NR, MB, MG and CV through electrostatic interaction and the adsorption capacities were 323.42, 235.18, 261.38 and 206.92 mg/g at 25°C , respectively. It was found that the pseudo-second-order kinetic model can well describe the adsorption kinetic of NR, MB, MG and CV. The adsorption was single layer adsorption according to the Langmuir model. Results of this work are of great significance for environmental applications of sodium titanate with low crystallinity as a promising adsorbent material used for dyeing water purification.

Acknowledgement

This work was supported by analysis and testing foundation of Jilin University and the National Natural Science Foundation of China (No. 51308252).

References

- [1] A. Ozturk, E. Malkoc. *Appl. Surf. Sci.* **299**, 105 (2014).
- [2] M. T. Yagub, T. K. Sen, S. Afroze, H.M. Ang. *Adv. Colloid Interface Sci.* **209**, 172 (2014).
- [3] P. Wang, M. Cao, C. Wang, Y. Ao, J. Hou, J. Qian. *Appl. Surf. Sci.* **290**, 116 (2014).
- [4] M. Rafatullah, O. Sulaiman, R. Hashim, A. Ahmad. *J. Hazard. Mater.* **177**, 70 (2010).
- [5] V. K. Gupta, R. Kumar, A. Nayak, T. A. Saleh, M. A. Barakat. *Adv. Colloid Interface Sci.* **193**, 24 (2013).
- [6] Y. Wang, G. Wang, H. Wang, C. Liang, W. Cai, L. Zhang. *Chem-Eur J.* **16**, 3497 (2010).
- [7] M. Visa, C. Bogatu, A. Duta. *Appl. Surf. Sci.* **256**, 5486 (2010).
- [8] D. V. Bavykin, F. C. Walsh. *Eur. J. Inorg. Chem.* 977 (2009).
- [9] N. Li, L. Zhang, Y. Chen, M. Fang, J. Zhang, H. Wang. *Adv. Funct. Mater.* **22**, 835 (2012).
- [10] H. Shi, X. Xiao, L. Zeng, Q. Zhang, J. Nan, L. Wang. *J Nanosci Nanotech.* **14**, 6934 (2014).
- [11] M. Plodinec, I. Friscic, D. Ivekovic, N. Tomasic, D. S. Su, J. Zhang. *J. Alloys Compd.* **499**, 113 (2010).
- [12] J. Huang, Y. Cao, Z. Liu, Z. Deng, W. Wang. *Chem. Eng. J.* **191**, 38 (2012).
- [13] M. Feng, W. You, Z. Wu, Q. Chen, H. Zhan. *ACS Appl. Mater & Inter.* **5**, 12654 (2013).
- [14] N. Chau Thanh, J. L. Falconer, D. Le Minh, W.-D. Yang. *Mater. Res. Bull.* **51**, 49 (2014).
- [15] I. El Saliby, L. Erdei, H. K. Shon, J. B. Kim, J.-H. Kim. *Catal. Today.* **164**, 370 (2011).
- [16] Y. Wu, M. Long, W. Cai, S. Dai, C. Chen, D. Wu, J. Bai. *Nanotechnology.* **20**, 185703 (2009).
- [17] S. H. V. R. J. Lacoste, J. C. Stone. *Anal. Chem.* **31**, 1246 (1959).
- [18] Y. Chen, N. Li, Y. Zhang, L. Zhang. *J. Colloid Interface Sci.* **422**, 9 (2014).
- [19] V. C. Ferreira, O. C. Monteiro. *J. Nanopart. Res.* **15**, (2013).
- [20] X.g. Zhao, J.g. Huang, B. Wang, Q. Bi, L.l. Dong, X.j. Liu. *Appl. Surf. Sci.* **292**, 576 (2014).
- [21] H. Ichinose, M. Terasaki, H. Katsuki. *J. Sol-Gel Sci. Technol.* **22**, 33 (2001).
- [22] M. Vithal, S. R. Krishna, G. Ravi, S. Palla, R. Velchuri, S. Pola. *Ceram. Int.* **39**, 8429 (2013).
- [23] J. Huang, Y. Cao, Z. Liu, Z. Deng, F. Tang, W. Wang. *Chem. Eng. J.* **180**, 75 (2012).
- [24] J. Huang, Y. Cao, Z. Deng, H. Tong. *J. Solid State Chem.* **184**, 712 (2011).
- [25] J. Huang, Y. Cao, M. Wang, C. Huang, Z. Deng, H. Tong, Z. Liu. **114**, 14748 (2010).
- [26] S. Xie, B. Zheng, Q. Kuang, X. Wang, Z. Xie, L. Zheng. *Crystengcomm.* **14**, 7715 (2012).
- [27] Y. Tang, Z. Jiang, Q. Tay, J. Deng, Y. Lai, D. Gong,

- Z. Dong, Z. Chen. *Rsc Advances*. **2**, 9406 (2012).
- [28] J. Ma, F. Yu, L. Zhou, L. Jin, M. Yang, J. Luan, Y. Tang, H. Fan, Z. Yuan, J. Chen. *Acs App Mater Inter*. **4**, 5749 (2012).
- [29] Y. W. L. Lim, Y. Tang, Y. H. Cheng, Z. Chen. *Nanoscale*. **2**, 2751 (2010).
- [30] H. Chen, J. Zhao. *Adsorption*. **15**, 381 (2009).
- [31] L. Xiong, Y. Yang, J. Mai, W. Sun, C. Zhang, D. Wei, Q. Chen, J. Ni. *Chem. Eng. J.* **156**, 313 (2010).
- [32] T. B. Musso, M. E. Parolo, G. Pettinari, F. M. Francisca. *J. Environ. Manage.* **146**, 50 (2014).

*Corresponding author: dlili104@sina.com